Multiple ionization and fragmentation of isolated pyrene and coronene molecules in collision with ions

A. Ławicki,[1] A. I. S. Holm,[2] P. Rousseau,[1,*] M. Capron,[1] R. Maisonny,[1] S. Maclot,[1] F. Seitz,[2] H. A. B. Johansson,[2] S. Rosén,[2] H. T. Schmidt,[2] H. Zettergren,[2] B. Manil,[3] L. Adoui,[1] H. Cederquist,[2] and B. A. Huber[1]

[1]*CIMAP (UMR 6252, CEA/CNRS/ENSICAEN/Université de Caen Basse-Normandie), Boulevard Henri Becquerel, BP5133, F-14070 Caen Cedex 5, France*
[2]*Department of Physics, Stockholm University, AlbaNova University Center, S-10691 Stockholm, Sweden*
[3]*Laboratoire de Physique des Lasers (UMR 7538, CNRS/Université Paris 13/Institut Galilée), 99 Avenue J. B. Clément, F-93430 Villetaneuse, France*
(Received 3 December 2010; published 8 February 2011)

The interaction of multiply charged ions (He^{2+}, O^{3+}, and Xe^{20+}) with gas-phase pericondensed polycyclic aromatic hydrocarbon (PAH) molecules of coronene ($C_{24}H_{12}$) and pyrene ($C_{16}H_{10}$) is studied for low-velocity collisions ($v \leqslant 0.6$ a.u.). The mass spectrometric analysis shows that singly and up to quadruply charged intact molecules are important reaction products. The relative experimental yields are compared with the results of a simple classical over-the-barrier model. For higher molecular charge states, the experimental yields decrease much more strongly than the model predictions due to the instabilities of the multiply charged PAH molecules. Even-odd oscillations with the number of carbon atoms, n, in the intensity distributions of the $C_nH_x^+$ fragments indicate a linear chain structure of the fragments similar to those observed for ion-C_{60} collisions. The latter oscillations are known to be due to dissociation energy differences between even- and odd-n C_n-chain molecules. For PAH molecules, the average numbers of H atoms attached to the C_nH_x chains are larger for even-n reflecting acetylenic bond systems.

I. INTRODUCTION

Polycyclic aromatic hydrocarbon molecules (PAHs) consist of joined aromatic carbon rings. They are formed as by-products in combustion processes and they are frequently present in soot material [1]. Due to the toxicity of some PAH molecules [2], their pollution is monitored [3]. Furthermore, PAH molecules are of particular interest in the fields of astrophysics and astrochemistry [4]. Many emission bands in the interstellar mid-infrared spectra are assigned to aromatic molecules, and therefore, PAH molecules are considered to be a major component of matter present in the interstellar medium. It is estimated that about 20% of the carbon in our galaxy is present in the form of PAH molecules [5,6].

PAH molecules are large π-electron systems which are strongly stabilized by the delocalization of the electrons. Two families can be distinguished—catacondensed PAHs and pericondensed PAHs—differing in the arrangement of the aromatic rings. In a pericondensed PAH, at least one carbon atom is a member of three rings and the molecules are more compact. As PAHs generally exhibit a planar geometry, pericondensed ones can be considered small hydrogen-saturated fragments of graphene.

Due to their astrophysical relevance, PAH molecules have been widely studied in the laboratory. The emission and absorption spectra of isolated molecules, in a matrix or in the gas phase have been measured (see Ref. [7] for a review). Photoionization [8] and photofragmentation of both neutral [9] and cationic [10] species have been studied. The irradiation of PAH molecules contained in condensed films

has also been performed with photons [11] and with proton beams [12]. However only recently, studies of the interaction of ions with PAH molecules in the gas phase have been made, concentrating on the ionization and fragmentation of linearly catacondensed anthracene ($C_{14}H_{10}$) monomers [13] and clusters [14]. Many of the experimental and theoretical studies are dedicated to the coronene ($C_{24}H_{12}$) molecule, which is formed by seven centrally condensed six-membered carbon rings representing a D_{6h} geometry. The smaller pyrene ($C_{16}H_{10}$) molecule is formed by four six-membered carbon rings. Coronene and pyrene are both pericondensed PAHs; their molecular structures are shown in Fig. 1.

In the interstellar medium, PAH molecules are exposed to a variety of ionizing processes. Many of these have been studied in the laboratory for both neutral and ionic species. Ionization potentials have been measured for coronene and pyrene by photoionization [8,15] and electron-impact ionization [15–18]. Recently, Penning ionization electron spectra of pyrene and coronene with metastable He atoms have been compared with ultraviolet photoelectron spectra [19]. The exposure to ionizing radiations can also lead to the fragmentation of the molecule, thus, the photodissociation spectra of the neutral molecules [9] and their cations [20,21] show the loss of hydrogen atoms and small hydrocarbon molecules. Surface-induced dissociation of pyrene has been measured at different energies [22] leading to multiple fragmentation into $C_nH_x^+$ series. The fragmentation of coronene and pyrene by collision-induced dissociation (CID) was widely studied for different energies [23–26]. Gas-phase fast atom bombardment of the molecules were performed with kilo–electron volt He and Ar [27,28]. Electron-impact mass spectrometric studies of coronene and pyrene molecules have been performed at different energies [16–18,29]. Two studies, both combining experiment and theory, have permitted

*prousseau@ganil.fr
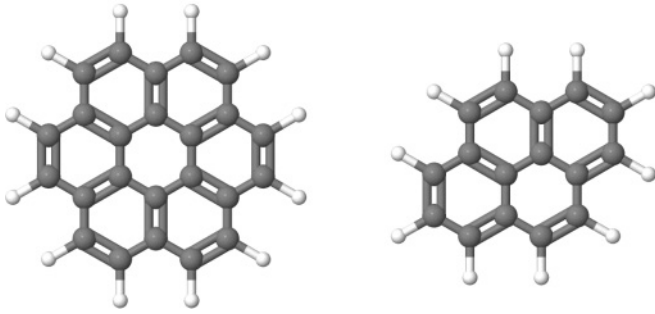
FIG. 1. Molecular structure of the coronene ($C_{24}H_{12}$) molecule (left) and of the pyrene ($C_{16}H_{10}$) molecule (right).

investigation in detail of the vibrational excitation of pyrene [30] and coronene [31]. The latter work also considers the low-energy electron attachment complementing the measurements presented in Ref. [32].

The aim of the present work is to extend the studies of PAH molecules of coronene and pyrene and to focus on collisions with slow multiply charged ions in different charge states (He^{2+}, O^{3+}, and Xe^{20+}). We discuss the present mass spectrometric results for collisions of multiply charged ions with coronene and pyrene molecules, with particular emphasis on the formation of intact multiply charged molecular cations, evaporation (i.e., emissions of neutral neutral particles) of hydrogen and small hydrocarbon molecules, and fragmentation in $C_nH_x^{q+}$ cations.

II. EXPERIMENTAL PROCEDURES

The experiment is performed in Caen at the low-energy ion beam facility ARIBE of GANIL. The experimental setup is described in detail elsewhere [33] and only a brief description is given here. Multiply charged ions are extracted from an electron cyclotron resonance ion source. The ion beam is mass-selected, pulsed, and transported to the experimental area. The ions collide with an effusive molecular beam produced by evaporation of the sample powder in an oven. Positively charged ionic products of the interaction are orthogonally extracted into a modified linear Wiley-McLaren time-of-flight mass spectrometer [34]. The residual background pressure in the interaction zone is 1×10^{-8} mbar, and during measurements a liquid nitrogen trap is used to further improve vacuum conditions (typically 3×10^{-9} mbar). We use commercial (Sigma Aldrich) coronene (97% purity) and pyrene (99% purity) powders without further purification. To obtain sufficient vapor densities the oven is heated to 190°C for coronene and to 60°C for pyrene. The mass-over-charge analyzed ionic products reach a Daly-type detector composed of a high-voltage conversion plate and a three-stage microchannel plate assembly for detecting the emitted electrons. This detection system allows for a uniform ion detection efficiency in the mass region of interest.

III. RESULTS AND DISCUSSION

A. Mass spectra

We have studied the interaction of O^{3+} and Xe^{20+} ions with coronene and pyrene at a velocity of 0.3 a.u. (6.3×10^5 m/s).

For the coronene molecule, additional measurements were also carried out with He^{2+} ions at a velocity of 0.55 a.u. (12.0×10^5 m/s). In Figs. 2 and 3, we show typical ion mass spectra obtained for the interaction of multiply charged ions with coronene and pyrene molecules, respectively. To compare the spectra, we normalize them to the maximum intensity of the intact molecular cation. In all cases, the dominant peaks are due to the formation of intact M^+ and M^{2+} cations, but also higher molecular charge states are visible. Furthermore, many small singly charged hydrocarbon fragments, $C_nH_x^+$, with n ranging up to $n = 11$, are created, as shown in the lower mass region in Figs. 2 and 3 (right panels). With increasing charge state of the projectile, the yields of the small fragments CH_x^+ and $C_2H_x^+$ increase strongly, indicating that they are due to charge-driven fragmentation processes. In contrast, larger $C_nH_x^+$ ions are important for He^{2+} projectiles and are most likely related to thermal fragmentation in processes where large amounts of energy are transferred to the molecule. The spectra also show doubly charged fragments $C_nH_x^{2+}$. Their intensities are higher for collisions with projectiles in higher charge states (Xe^{20+}) as probabilities for multiple electron removal become higher. In the case of pyrene, an intense narrow peak at the position ($m/z = 88$ amu) is observed, which is identified as being due to doubly charged ions $C_{14}H_8^{2+}$. The origin of this decay channel is discussed in detail in Sec. III D.

B. Multiply charged molecular cations

Peaks corresponding to the intact multiply charged molecular ions M^{r+} have been integrated and normalized to the yields of the corresponding singly charged molecules. The relative intensities of the (multiply charged) cations (including the H losses) are plotted in Fig. 4 as a function of their charge state for collisions of Xe^{20+} ions with different targets. We include the H-loss peaks in these yields, as these channels are strongly dominated by evaporation of the (multiply) charged intact molecule and are not due to fission processes emitting charged fragments. This allows us to compare the experimental values with the results obtained from the classical over-the-barrier (COB) model [35] for point-like targets. The COB model gives the sequences of critical distances for electron transfer of the $(r + 1)$-th electron from the target molecules PAH^{r+} [35]:

$$R_{r+1} = [2(q - r)^{1/2}(r + 1)^{1/2} + (r + 1)]/I_{r+1}$$

where q is the projectile charge state and I_{r+1} is the ionization energy of PAH^{r+}. Here, we used recent high-level density functional theory calculations of the vertical ionization energies, which follow linear dependencies as functions of r, $I_{r+1} = 7.18 + 4.91r$ eV (anthracene), $I_{r+1} = 7.02 + 4.84r$ eV (pyrene), and $I_{r+1} = 6.70 + 4.05r$ eV (coronene) [36]. This gives, for example, $R_1 = 37.7$ a_0 (anthracene), $R_1 = 38.6$ a_0 (pyrene), and $R_1 = 40.4$ a_0 (coronene), corresponding to total cross sections for electron removal and fragmentation of $\sigma_{tot} = \pi R_1^2 \approx 4.5 \times 10^3$ a_0^2 (anthracene), $\sigma_{tot} \approx 4.7 \times 10^3$ a_0^2 (pyrene), and $\sigma_{tot} \approx 4.9 \times 10^3$ a_0^2 (coronene). These values may be compared with the geometrical dimensions of the three molecules of roughly 180 a_0^2 (anthracene), 220 a_0^2 (pyrene), and 260 a_0^2 (coronene). Thus, electron transfers proceed at a large distance compared to the molecule size.
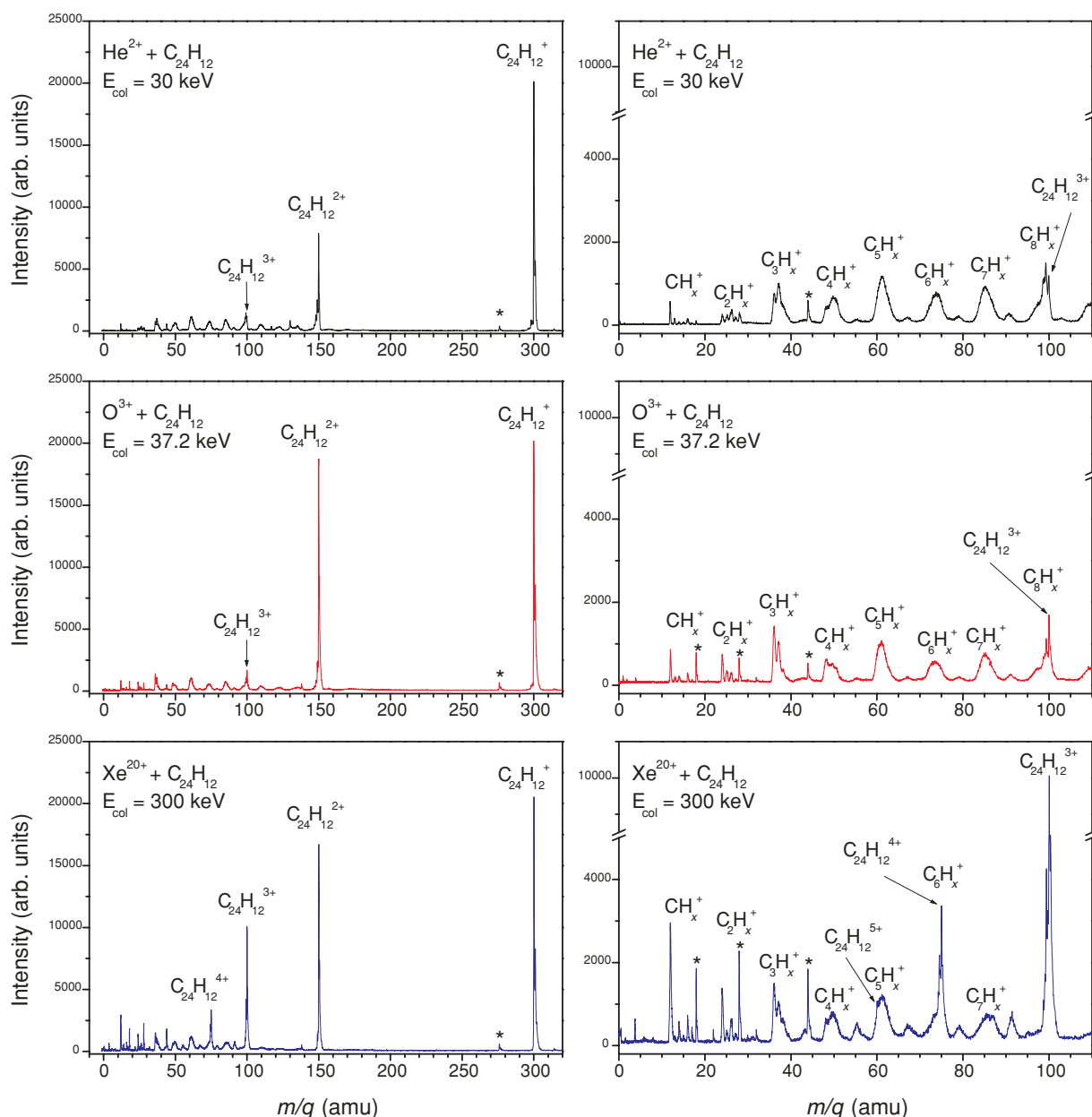
FIG. 2. (Color online) Mass spectra of ionic products of the interaction of multiply charged ions with a molecule of coronene $C_{24}H_{12}$ ($m = 300$ amu). Right panels show zoom-ins on the low-mass region. Peaks marked with a star are due to residual gas and to powder contaminations.

The COB model relative yields (σ_{r+1}/σ_1) for electron removal, shown in Fig. 4, were extracted from the differences in the geometrical cross sections, $\sigma_{r+1} = \pi(R_{r+1}^2 - R_{r+2}^2)$. The model results follow exponential decreasing trends as functions of PAH charge state reflecting the slopes of the ionization energy sequences, where the less steep trend belongs to coronene, while anthracene and pyrene display similar and much steeper behaviors.

The model and experimental results agree well for production of up to triply charged coronene and doubly charged pyrene and anthracene, while the measured intensities are significantly lower than the model intensities for more highly charged species, suggesting that then decay pathways other

than H losses become important processes. Thus, the larger deviations with decreasing PAH size point at an increased propensity for fragmentation, reflecting that the larger PAH molecules may accommodate more charges and excitation energy without fragmenting on the experimental time scales (μs).

The present measurements yield $r = 4$ for pyrene and $r = 4$ or possibly $r = 5$ for coronene as the highest charge state for nonfragmenting (metastable) molecular cations following collisions with Xe^{20+}. Recent high-level calculations show that pyrene and coronene are thermodynamically unstable for charge states exceeding 3 and 4, respectively [36]. However, as in the case of C_{60} fullerenes [37–42], fission barriers
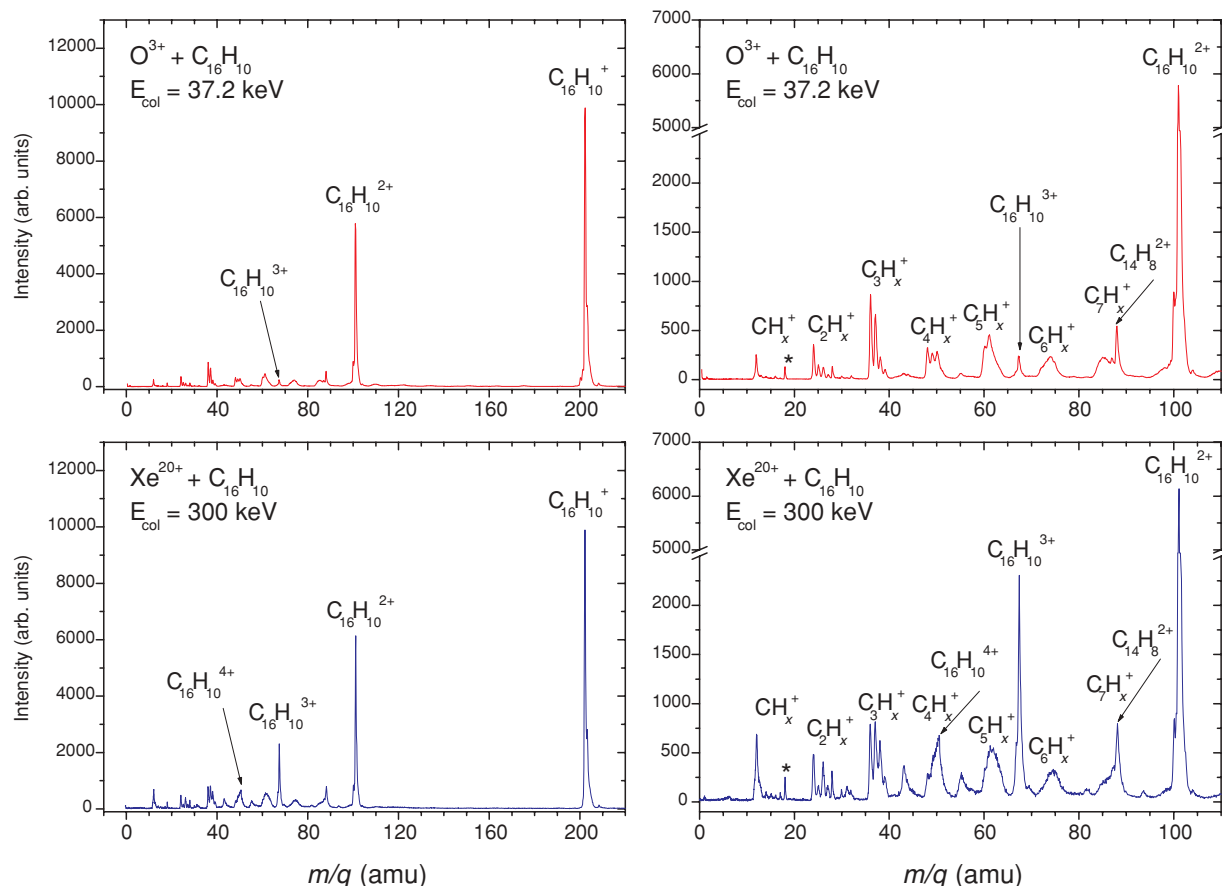
FIG. 3. (Color online) Mass spectra of ionic products of the interaction of multiply charged ions with a molecule of pyrene $C_{16}H_{10}$ ($m = 202$ amu). Right panels show zoom-ins on the low-mass region. Peaks marked with a star are due to residual gas and to powder contaminations.

should prevent even more highly charged species from prompt decay. The present experiments show that $C_{16}H_{10}^{4+}$ may be stable on the microsecond time scale, and at the position
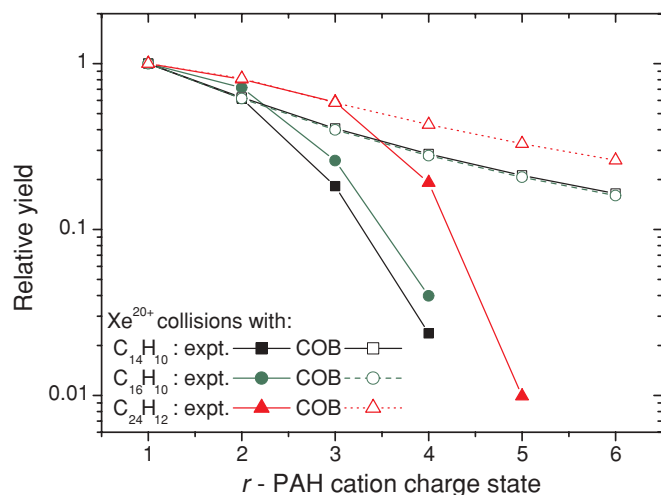
FIG. 4. (Color online) Experimental relative yields (filled symbols) of molecular cations PAH^{r+} (including the intensities in the H-loss channels) as functions of their charge state after Xe^{20+} collisions with coronene $C_{24}H_{12}$, pyrene $C_{16}H_{10}$, and anthracene $C_{14}H_{10}$. The corresponding COB model results (see text) are displayed by open symbols.

expected for $C_{24}H_{12}^{5+}$ a small feature is present. The presently observed critical PAH charge state and multiply charged cations relative intensities are higher than those previously observed for coronene and pyrene using other ionization methods [18,28,43]. Recently, Yatsuhashi and Nakashima observed a high relative yield of multiply charged PAHs (up to 4+) using intense femtosecond-laser pulses [44], but these studies did not include pyrene or coronene.

From the difference between the COB model ionization yields and the measured yields of intact ions (now excluding the intensities of the H-loss channels), we evaluate total "fragmentation" yields for given molecular cation charge states through $(Y_{COB} - Y_{expt})/Y_{COB}$, where Y_{expt} is the measured yield and Y_{COB} is the yield expected from the COB model. This is thus an estimate of the instability of the corresponding molecular cation for a given charge state after the interaction with Xe^{20+}. To discuss the effect of the molecular geometry on the stability of the molecular cations, we compare the fragmentation yield for collisions of Xe^{20+} on the catacondensed molecule of anthracene ($C_{14}H_{10}$) and the pericondensed molecule of pyrene ($C_{16}H_{10}$). We consider these two molecules, as their sizes are rather similar. In Fig. 5, we plot semiempirical fragmentation yields showing that the pericondensed pyrene molecule is more stable than the catacondensed anthracene molecule for a given charge state.
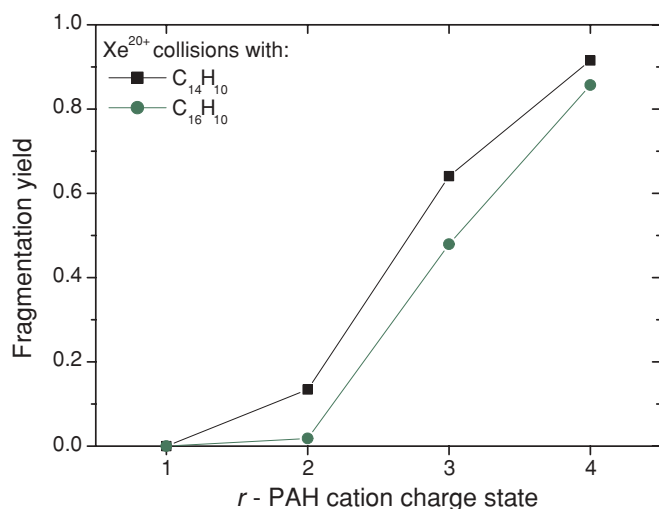
FIG. 5. (Color online) Semiempirical fragmentation yields (see text) as functions of the molecular cation charge state for pericondensed pyrene ($C_{16}H_{10}$) and catacondensed anthracene ($C_{14}H_{10}$) after collisions with Xe^{20+} ions.

C. Hydrogen loss

In Fig. 6 we show zoom-ins on the regions of the singly and doubly charged coronene molecules produced in collisions with He^{2+} ions at 30 keV and Xe^{20+} ions at 300 keV. The peaks are structured to the right due to the carbon isotopes (^{12}C and ^{13}C) and to the left, depending on the individual case, by the loss of hydrogen atoms. Concerning the loss of hydrogen atoms, the four spectra clearly show that the evaporation yield and the length of the observed evaporation chain depend strongly on the charge state of the projectile. This is due to the energy transfer during the collision, which is lower for higher projectile charge states for a given ionization process. For single ionization of the coronene molecule by Xe^{20+} collisions, the energy transfer is very low, as the transfer mostly occurs at very large internuclear distances ($\approx$40 a.u.), and no evaporation of H atoms is observed. This is different
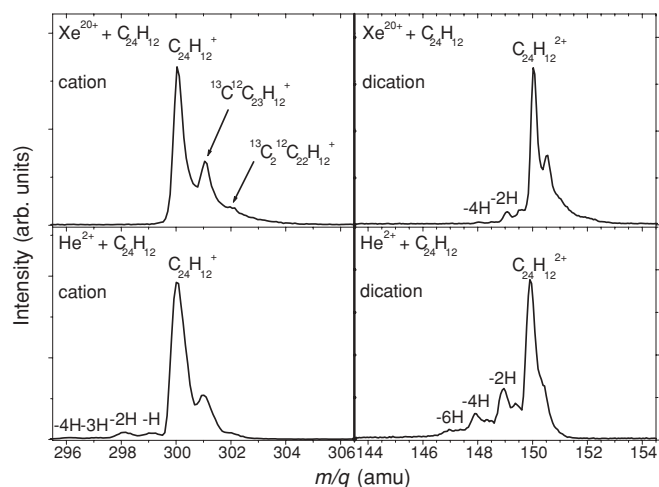
FIG. 6. Peak forms of singly (left panels) and doubly (right panels) charged coronene ions. Upper panels, Xe^{20+} projectiles; lower panels, He^{2+} projectiles.
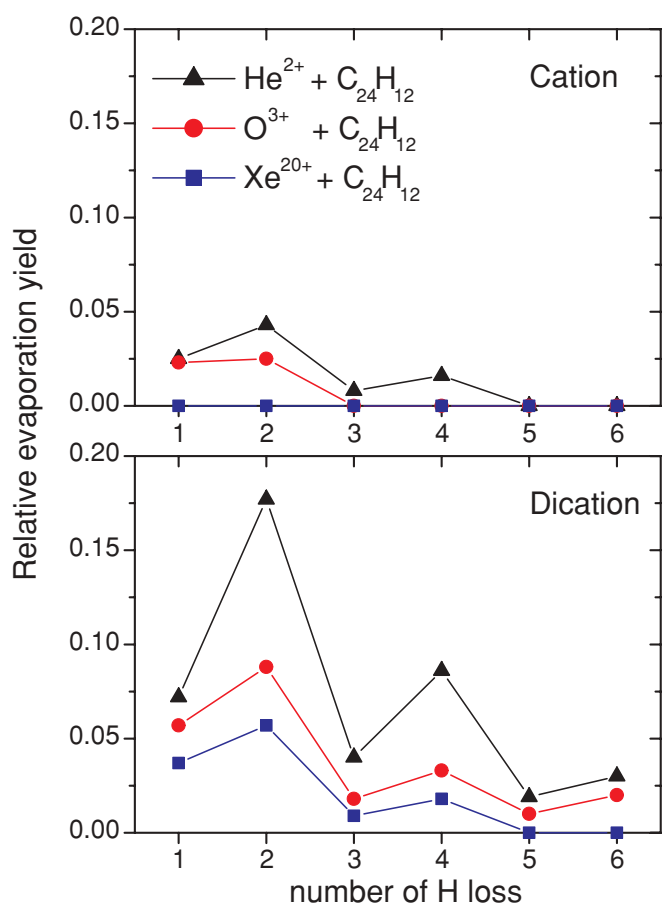
FIG. 7. (Color online) Relative yields for losses of one to six hydrogen atoms from singly and doubly charged coronene produced in collisions with three different projectiles.

when He^{2+} ions are used. The internal energy of the produced molecular ion increases due to the smaller characteristic impact parameter, and losses of from one to four H atoms are observed. The number of lost H atoms as well as the relative intensities increase when doubly charged molecules are produced. In the case of He^{2+} projectiles, up to six H atoms are lost.

The relative yields for losses of one to six H atoms from singly and doubly charged coronene produced in collisions with He^{2+}, O^{3+}, and Xe^{20+} are displayed in Fig. 7. To extract these values, we have taken into account the isotopic distribution and a system of coupled population equations has been solved assuming that the rates for the respective decay processes do not depend on the isotopic composition of the molecule. We note that there is an oscillating behavior favoring the emission of even numbers of H atoms. Moreover, the even-to-odd ratios (i.e., the ratios of the sums of the intensities from emissions of even and odd numbers of H atoms) increases with the final charge state of the molecular cation and with increasing internal energy (decreasing projectile charge state). For cations these even-to-odd ratios are 1.79 for He^{2+} and 1.09 for O^{3+}, and for the dications they increase to 2.24 for He^{2+}, 1.66 for O^{3+}, and 1.63 for Xe^{20+}. Thus, emissions of even numbers of H atoms are favored, in particular, when high energies are transferred.

The importance of C-H cleavage processes has been discussed frequently in the literature [9,18,20,21,25,32,45]. It is clear that for a given internal energy of the system, the C-H cleavage is favored with respect to C-C cleavage due to the weaker bond strength in the former case. In particular, the complete dehydrogenation of coronene may be reached by photoionization without breaking any of the C-C bonds [20]. In most cases, it is found that the emission of an even number of H atoms is favored. The question arises if this is due to the emission of two separate H atoms or one H_2 molecule. Jochims *et al.* [9] showed, by threshold photoionization measurements, that the emission of H_2 molecules may dominate for higher internal energies. *Ab initio* calculations of excited naphthalene cations ($C_{10}H_8^+$) suggest that H_2 emissions are initiated by single or multiple hydrogen shifts to neighboring carbon atoms where H_2 molecules are formed, and that the branching ratio for H_2 loss increases when the internal energy of the molecules increases [46]. Thus, as we find that the preference for loss of even numbers of H atoms increases with increasing energy transfers (lower projectile charge state and/or double ionization of the PAH molecule), it appears that molecular H_2 loss is an important channel also under the present experimental conditions.

D. Loss of neutral and charged C_nH_x molecules

In addition to the loss of H atoms, for some PAH molecules the evaporation of larger neutral systems has been observed. For example, in photodissociation and low-energy CID studies of pyrene, the emission of acetylene molecules C_2H_2 was reported [9,25]. Furthermore, for different small PAHs (up to four fused rings), Kingston *et al.* [43] observed that a charge separation occurs for doubly and triply charged cations, leading to the formation of CH_3^+, $C_2H_2^+$, and $C_3H_3^+$ ions and other charged products. In the case of pyrene an additional decay pathway results in the loss of $C_4H_2^+$. For ions colliding with anthracene, losses of C_2H_2 and C_4H_2, sometimes accompanied by additional H losses, have been observed [13,14].

For multiply charged ions colliding with coronene, no such channels have been identified. In the case of pyrene, we assigned the peak at $m/q = 88$ to the loss of one acetylene unit from the doubly charged molecular ion (see Fig. 3, lower part). This channel seems to be present in the femtosecond-laser ionization mass spectrum in Ref. [47]. We also observe that the resulting $[M-C_2H_2]^{2+}$ ion may dissociate further by H loss. A part of the $C_{14}H_8^{2+}$ product could also be due to fission of the M^{3+} molecule, as the $C_2H_2^+$ ion signal is rather high compared to that of other $C_2H_x^+$ ions. In the case of the collision of O^{3+} with pyrene, we observe weak signals at $m/q = 176$, 163, and 152. These peaks correspond to the loss of C_2H_2, C_3H_3, and C_4H_2, respectively. Again, fission processes involving the doubly charged dication may contribute to the observed intensity. In contrast with other ionization methods [9,25,29], the C_nH_x losses here are minor decay channels, as interactions with multiply charged ions are more gentle.

Recent calculations of the dissociation energies for losses of H, H^+, C_2H_2, and $C_2H_2^+$ for five PAH molecules in different charge states [36] show that the channel linked to the emission of neutral hydrogen is energetically favored with respect to

other dissociation channels for neutral, singly charged, and doubly charged coronene and pyrene. For PAH charge states exceeding $r = 2$, the lowest dissociation energies correspond to fission processes (H^+ or $C_2H_2^+$ loss). These theoretical predictions are in agreement with the experimental results already described.

E. Fragmentation into singly and doubly charged C_nH_x molecules

Apart from losses of hydrogen and small C_nH_x molecules, the fragmentation of coronene or pyrene results in a wide series of $C_nH_x^{q+}$ cations, which may be singly or doubly charged (see Figs. 2 and 3). In the case of He^{2+} projectiles colliding with coronene, the size distribution of the $C_nH_x^+$ fragments extends up to $n = 15$, whereas for O^{3+} and Xe^{20+} ions the distribution ends at $n = 12$ and 11, respectively (see Fig. 8). The $C_nH_x^{q+}$ fragments may have two different origins. In the case of He^{2+}, the fragment distribution is governed by an appreciable energy transfer occurring at small impact parameters, which finally leads to the dissociation into large fragments. In the case of higher projectile charges, the fragmentation is mainly due to charge separation processes of multiply charged molecular cations.
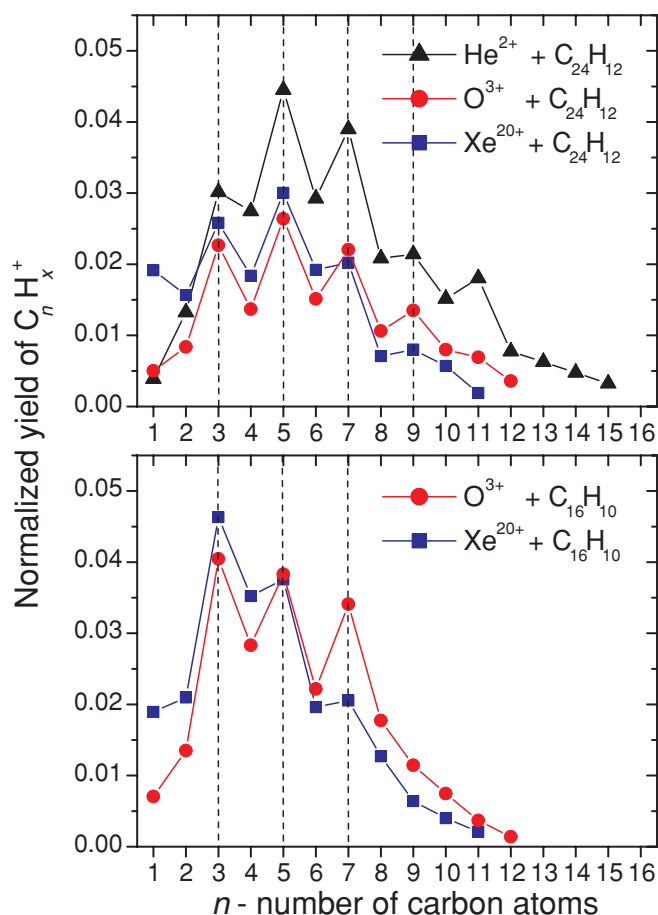
FIG. 8. (Color online) Normalized yield of $C_nH_x^+$-fragments as a function of n. Intensities have been integrated for different x values. Upper panel, coronene; lower panel, pyrene.

One striking feature of the fragmentation spectra is the observed even-odd oscillations in intensity of the $C_nH_x^+$ fragments as a function of the number n of carbon atoms. As shown in Fig. 8, fragments containing odd numbers of carbon atoms are more frequent than even ones. Such behavior is also observed in ion-anthracene collisions [13]. Similar observations of even-odd oscillations with the number of carbon atoms have also been reported for ion-induced fragmentation of fullerene molecules (see, e.g., Ref. [48]).

Small C_nH_x molecules, with $x = 1,2$, are believed to have geometrical structures similar to pure carbon clusters C_n [13,49]. In general, small and intermediate C_n clusters may have a large variety of structures, including linear chains, mono- and polycyclic rings, and even small fullerenes, depending on their size (for a review see Ref. [50]). Carbon clusters smaller than C_{10} are often linear, either with a cumulenic bonding : $C = C \cdots C = C$:, characterized by nearly equivalent bond lengths, or with an acetylenic bonding $\cdot C \equiv C - C \cdots C - C \equiv C \cdot$, with alternating bond lengths [50]. Odd-numbered chains have a cumulenic bond system with a $^1\Sigma_g^+$ electronic ground state, whereas even-numbered chains may show both types of bonding corresponding to a $^3\Sigma_g^-$ ground state. However, in particular for small chain lengths, the acetylenic forms of even-numbered linear chains are energetically higher than the cumulenic configurations. Properties like electron attachment energies, ionization potentials, and dissociation energies depend strongly on the number of carbon atoms contained in the chain, that is, on the bond character, and odd-numbered chains are in general more stable. The dissociation energies for singly charged ions C_3^+, C_5^+, and C_7^+ are in the range between 6 and 6.5 eV, whereas for the even ones, C_2^+, C_4^+, and C_6^+, the corresponding values are between 5 and 5.5 eV [50]. This difference readily explains the oscillations shown in Fig. 8 and it is thus indeed likely that the small C_nH_x fragments observed here are linear-chain molecules. This is also the conclusion drawn by Postma *et al.* [13], who studied ion collisions on anthracene.

In the cases of even-numbered $C_nH_x^+$ fragments, the average numbers of hydrogen attached are larger than for odd-numbered fragments. This may be for two reasons. Charge separation reactions of multiply charged PAH molecules lead preferentially to the emission of $C_2H_2^+$ and $C_4H_2^+$ [43], thus contributing to even-n $C_nH_x^+$ products. In addition, as the odd-numbered carbon chains have a cumulenic bond structure with less reactive ends, similarly a lower degree of hydrogenation is expected [13].

IV. SUMMARY AND CONCLUSIONS

We have studied kilo–electron volt collisions between multiply charged ions (He^{2+}, O^{3+}, and Xe^{20+}) and the PAH molecules coronene and pyrene. In frontal and small impact parameter collisions, large amounts of energy are transferred, leading to multiple ionization and multifragmentation. This gives singly and doubly charged, small C_nH_x fragments with

even-odd oscillations in the intensity distributions as functions of n. This trend and the higher average hydrogenation for even-n compared to odd-n fragments indicate linear-chain structures with cumulenic (odd-n) and acetylenic (even-n) bond systems.

In more distant collisions, singly and multiply charged intact PAH^{r+} may be produced sufficiently cold to survive experimental time scales of microseconds. The present experimental stability limits correspond to $r = 4$ and $r = 4$ (or 5) for pyrene and coronene, respectively. For low projectile charge states, multiply charged PAHs may emit up to six H atoms. The preference for loss of an even number of H atoms suggests that molecular H_2 emission is a competitive decay pathway for higher internal PAH temperatures. In the pyrene case, C_2H_2 emission from $C_{16}H_{10}^{2+}$ and/or $C_2H_2^+$ emission from $C_{16}H_{10}^{3+}$ also compete with the H-loss channels. These results are consistent with recent high-level calculations investigating the stabilities and decay pathways of singly and multiply charged cations of five PAH molecules including pyrene and coronene [36].

The present experimental relative multiple ionization yields (including the H-loss channels) follow decreasing trends as functions of PAH charge states. For low charge states, these results are in agreement with predictions based on a simple COB model in which the geometrical structure of the molecule as well as the capture of more tightly bound inner electrons is ignored, while there are much steeper decreasing trends in the experimental yield when the PAHs reach their thermodynamical stability limits, where fragmentation processes other than H losses have to be taken into account. In the case of anthracene and pyrene molecules, it is found that the pericondensed form (pyrene) is more stable in kilo–electron volt ion-PAH collisions. To shed further light on the intriguing stability issues of (multiply) ionized PAHs, multicoincidence experiments similar to the ones for ion-fullerene collision [37,38,41,51] and high-level calculations of fission barriers [42] are needed. Further model developments in which the actual PAH molecular structures are taken into account would be useful. Still the favorable comparisons between the simple version of the over-the-barrier model, presently used, and the measured relative single and multiple PAH ionization cross sections indicates an easy way to estimate absolute electron transfer cross sections and rate coefficients for PAH molecules colliding with kilo–electron volt ions.

[1] H. Richter and J. B. Howard, Prog. Energy Combust. Sci. **26**, 565 (2000).

[2] P. Boffetta, N. Jourenkova, and P. Gustavsson, Cancer Causes Control **8**, 444 (1997).

[3] K. Srogi, Environ. Chem. Lett. **5**, 169 (2007).

[4] A. G. G. M. Tielens, Annu. Rev. Astron. Astrophys. **46**, 289 (2008).

[5] A. Li and B. T. Draine, Astrophys. J. **554**, 778 (2001).

[6] C. Joblin and G. Mulas, EAS Publ. Ser. **35**, 133 (2009).

[7] J. Oomens, A. G. G. M. Tielens, B. G. Sartakov, G. von Helden, and G. Meijer, Astrophys. J. **591**, 968 (2003).

[8] S. Tobita, S. Leach, H. W. Jochims, E. Rühl, E. Illenberger, and H. Baumgärtel, Can. J. Phys. **72**, 1060 (1994).

[9] H. W. Jochims, E. Rühl, H. Baumgärtel, S. Tobita, and S. Leach, Astrophys. J. **420**, 307 (1994).

[10] J. Oomens, A. J. A. van Roij, G. Meijer, and G. von Helden, Astrophys. J. **542**, 404 (2000).

[11] M. P. Bernstein, S. A. Sandford, L. J. Allamandola, J. S. Gillette, S. J. Clemett, and R. N. Zare, Science **283**, 1135 (1999).

[12] M. P. Bernstein, M. H. Moore, J. E. Elsila, S. A. Sandford, L. J. Allamandola, and R. N. Zare, Astrophys. J. **582**, L25 (2003).

[13] J. Postma, S. Bari, R. Hoekstra, A. G. G. M. Tielens, and T. Schlathölter, Astrophys. J. **708**, 435 (2010).

[14] A. I. S. Holm, H. Zettergren, H. A. B. Johansson, F. Seitz, S. Rosén, H. T. Schmidt, A. Ławicki, J. Rangama, P. Rousseau, M. Capron, R. Maisonny, L. Adoui, A. Méry, B. Manil, B. A. Huber, and H. Cederquist, Phys. Rev. Lett. **105**, 213401 (2010).

[15] D. Schröder, J. Loss, H. Schwarz, R. Thissen, D. V. Preda, L. T. Scott, D. Caraiman, M. V. Frach, and D. K. Böhme, Helv. Chim. Acta **84**, 1625 (2001).

[16] M. E. Wacks, J. Chem. Phys **41**, 1661 (1964).

[17] E. J. Gallegos, J. Phys. Chem. **72**, 3452 (1968).

[18] S. Denifl, B. Sonnweber, J. Mack, L. T. Scott, P. Scheier, K. Becker, and T. D. Märk, Int. J. Mass Spectrom. **249**, 353 (2006).

[19] Y. Yamakita, M. Yamauchi, and K. Ohno, J. Chem. Phys. **130**, 024306 (2009).

[20] S. P. Ekern, A. G. Marshall, J. Szczepanski, and M. Vala, Astrophys. J. **488**, L39 (1997).

[21] S. P. Ekern, A. G. Marshall, J. Szczepanski, and M. Vala, J. Phys. Chem. A **102**, 3498 (1998).

[22] M. E. Bier, J. C. Schwartz, K. L. Schey, and R. G. Cooks, Int. J. Mass Spectrom. Ion Processes **103**, 1 (1990).

[23] B. Shushan and R. K. Boyd, Org. Mass Spectrom. **15**, 445 (1980).

[24] B. D. Nourse, K. A. Cox, K. L. Morand, and R. G. Cooks, J. Am. Chem. Soc. **114**, 2010 (1992).

[25] X. Wang, H. Becker, A. C. Hopkinson, R. E. March, L. T. Scott, and D. K. Böhme, Int. J. Mass Spectrom. Ion Processes **161**, 69 (1997).

[26] R. Arakawa, M. Kobayashi, and T. Nishimura, J. Mass Spectrom. **35**, 178 (2000).

[27] M. Takayama, Int. J. Mass Spectrom. Ion Processes **121**, R19 (1992); J. Am. Soc. Mass Spectrom. **6**, 114 (1995).

[28] M. Takayama, Int. J. Mass Spectrom. Ion Processes **152**, 1 (1996).

[29] P. J. Linstrom and W. G. Mallard, eds., NIST Chemistry WebBook, NIST Standard Reference Database Number 69 (National Institute of Standards and Technology, Gaithersburg, MD), [http://webbook.nist.gov/].

[30] M. Baba, M. Saitoh, Y. Kowaka, K. Taguma, K. Yoshida, Y. Semba, S. Kasahara, T. Yamanaka, Y. Ohshima, Y.-C. Hsu, and S. H. Lin, J. Chem. Phys. **131**, 224318 (2009).

[31] R. Abouaf and S. Díaz-Tendero, Phys. Chem. Chem. Phys. **11**, 5686 (2009).

[32] S. Denifl, S. Ptasińska, B. Sonnweber, P. Scheier, D. Liu, F. Hagelberg, J. Mack, L. T. Scott, and T. D. Märk, J. Chem. Phys. **123**, 104308 (2005).

[33] T. Bergen, X. Biquard, A. Brenac, F. Chandezon, B. A. Huber, D. Jalabert, H. Lebius, M. Maurel, E. Monnand, J. Opitz, A. Pesnelle, B. Pras, C. Ristori, and J. C. Rocco, Rev. Sci. Instrum. **70**, 3244 (1999).

[34] F. Chandezon, B. Huber, and C. Ristori, Rev. Sci. Instrum. **65**, 3344 (1994).

[35] A. Bárány, G. Astner, H. Cederquist, H. Danared, S. Huldt, P. Hvelplund, A. Johnson, H. Knudsen, L. Liljeby, and K.-G. Rensfelt, Nucl. Instrum. Methods Phys. Res. B **9**, 397 (1985).

[36] A. I. S. Holm, H. A. B. Johansson, H. Cederquist, and H. Zettergren, J. Chem. Phys. **134**, 044301 (2011).

[37] H. Cederquist, J. Jensen, H. T. Schmidt, H. Zettergren, S. Tomita, B. A. Huber, and B. Manil, Phys. Rev. A **67**, 062719 (2003).

[38] S. Tomita, H. Lebius, A. Brenac, F. Chandezon, and B. A. Huber, Phys. Rev. A **67**, 063204 (2003).

[39] P. Scheier, B. Dünser, and T. D. Märk, Phys. Rev. Lett. **74**, 3368 (1995).

[40] G. Senn, T. D. Märk, and P. Scheier, J. Chem. Phys **108**, 990 (1998).

[41] S. Martin, L. Chen, R. Brédy, J. Bernard, M. C. Buchet-Poulizac, A. Allouche, and J. Désesquelles, Phys. Rev. A **66**, 063201 (2002).

[42] S. Díaz-Tendero, M. Alcamí, and F. Martín, Phys. Rev. Lett. **95**, 013401 (2005).

[43] R. G. Kingston, M. Guilhaus, A. G. Brenton, and J. H. Beynon, Org. Mass Spectrom. **20**, 406 (1985).

[44] T. Yatsuhashi and N. Nakashima, J. Phys. Chem. A **114**, 7445 (2010).

[45] C. Pech, P. Boissel, M. Armengaud, P. Frabel, and C. Joblin, EAS Publ. Ser. **4**, 297 (2002).

[46] Y. A. Dyakov, C.-K. Ni, S. H. Lin, Y. T. Lee, and A. M. Mebel, Phys. Chem. Chem. Phys. **8**, 1404 (2006).

[47] L. Robson, K. W. D. Ledingham, A. D. Tasker, P. McKenna, T. McCanny, C. Kosmidis, D. A. Jaroszynski, D. R. Jones, R. C. Issac, and S. Jamieson, Chem. Phys. Lett. **360**, 382 (2002).

[48] J. Opitz, H. Lebius, B. Saint, S. Jacquet, B. A. Huber, and H. Cederquist, Phys. Rev. A **59**, 3562 (1999).

[49] J. R. Heath, Q. Zhang, S. C. O'Brien, R. F. Curl, H. W. Kroto, and R. E. Smalley, J. Am. Chem. Soc. **109**, 359 (1987).

[50] A. van Orden and R. J. Saykally, Chem. Rev. **98**, 2313 (1998).

[51] L. Chen, S. Martin, J. Bernard, and R. Brédy, Phys. Rev. Lett. **98**, 193401 (2007).